XLIII CILAMCE
21–25, November, 2022
FOZ DO IGUAÇU – PR – BRAZIL

An Efficiency Study of the Radial Polynomial Expansion Method for Solving Singular Integrals in the Dual-BEM

Beatriz B. F. Fonseca[1], Rodrigo G. Peixoto[1]

[1]*Post-Graduate Program in Structural Engineering, Federal University of Minas Gerais*
Av. Pres. Antônio Carlos, 6627 - Pampulha, 31270-901, Belo Horizonte - MG, Brazil
beatrizbffonseca@gmail.com, rodrigo.peixoto@dees.ufmg.br

Abstract. In the Boundary Element Method (BEM), when the element which is being integrated contains the source point, singularities arise in the integrals that govern the problem. Although several classical methods have already been proposed and successfully used, their numerical implementation is laborious and often requires particular codes for each type integral kernel. Recently, a method that allows the solution of integrals with different singularity orders in a single numerical procedure has been proposed. It is based on the polynomial expansion of the radial distance between the source and field points and it is called here as Radial Polynomial Expansion Method (RPEM). The RPEM has its efficiency studied for application to the Dual-BEM. Elements with quadratic interpolation functions are analyzed. The efficiency is verified in terms of the element distortion and the number of terms needed in the expansion. For this, the method is implemented in a computational code in Fortran 95 and the results are compared with other formulations, such as the singularity subtraction method. Once the reliability and applicability of the method have been proven, it is intended to apply the solutions found in a Dual-BEM code, for the analysis of fatigue crack propagation.

Keywords: Singular Integrals, Radial Polynomial Expansion Method, Dual Boundary Element Method

1 Introduction

The Boundary Element Method (BEM) has been successfully applied to crack propagation problems, having as an advantage, in relation to the standard Finite Element Method the capacity of the mesh to follow the crack growth, without the need to re-mesh the domain at each crack increment.

For the analysis of general cracks, it is necessary to apply the Dual Boundary Element Method (DBEM). The theoretical bases of DBEM were proposed by Hong and Chen [1] and the method was later systematized for application to fracture mechanics problems by Portela et al. [2, 3, 4]. The method consists of applying the displacement boundary integral equation on one of the crack faces, while the traction boundary integral equation is applied on the opposite face, which is presented in Fig. 1. The displacement equation is applied to the rest of the boundary, as proposed by Portela et al. [3].

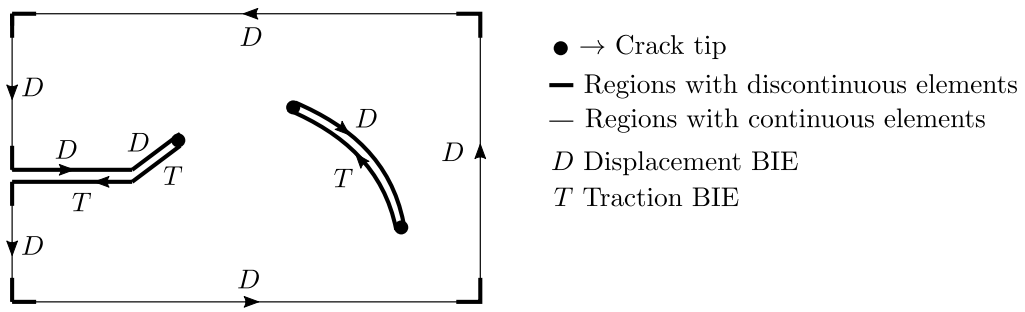

Figure 1. Strategy for boundary discretization in the application of the Dual Boundary Element Method

The boundary integral equations (BIE) that are applied in DBEM are:

- BIE for displacement at boundary points ($\xi \in \Gamma$):

$$\frac{1}{2}u_j\left(\boldsymbol{\xi}\right) + \int\!\!\!\!\!\!\diagup_{\Gamma} t_{ij}^{*}\left(\boldsymbol{\xi},\boldsymbol{x}\right) u_j\left(\boldsymbol{x}\right) d\Gamma = \int_{\Gamma} u_{ij}^{*}\left(\boldsymbol{\xi},\boldsymbol{x}\right) t_j\left(\boldsymbol{x}\right) d\Gamma; \tag{1}$$

- BIE for traction at boundary points ($\xi \in \Gamma$):

$$n_i\left(\boldsymbol{\xi}\right) \int\!\!\!\!\!\!\diagup_{\Gamma} u_{ijk}^{*}\left(\boldsymbol{\xi},\boldsymbol{x}\right) t_k(\boldsymbol{x}) d\Gamma - \frac{1}{2} t_j\left(\boldsymbol{\xi}\right) = n_i\left(\boldsymbol{\xi}\right) \int\!\!\!\!\!\!\!\diagup\!\!\!\diagup_{\Gamma} t_{ijk}^{*}\left(\boldsymbol{\xi},\boldsymbol{x}\right) u_k(\boldsymbol{x}) d\Gamma. \tag{2}$$

Where, Γ denotes the boundary, $\boldsymbol{\xi}$ is the source point, $\boldsymbol{x}$ refers to the analysed field point, u_i refers to the displacement components, and t_i to the traction components, i, j and k refer to the Cartesian components, which assume values 1 and 2 for the two-dimensional case and 1, 2 and 3 for the three-dimensional case, n_i denotes the external unitary normal vector to Γ, the symbols $\int\!\!\!\!\!\!\diagup$ and $\int\!\!\!\!\!\!\!\diagup\!\!\!\diagup$ indicate that the integrals exist only, respectively, in the senses of the Cauchy principal value and the Hadamard principal value and $u_{ij}^{*}\left(\boldsymbol{\xi},\boldsymbol{x}\right)$, $t_{ij}^{*}\left(\boldsymbol{\xi},\boldsymbol{x}\right)$, $u_{ijk}^{*}\left(\boldsymbol{\xi},\boldsymbol{x}\right)$ and $t_{ijk}^{*}\left(\boldsymbol{\xi},\boldsymbol{x}\right)$ represent Kelvin fundamental solution terms, which can be found in many BEM books, e.g., Brebbia et al. [5], Brebbia [6], Aliabadi [7] and Katsikadelis [8].

These integrals presented in eq. (1) and eq. (2) are regular, when the source point does not belong to the element being integrated and, therefore, can be solved by the Gauss-Legendre quadrature. However, when the source point belongs to the element being integrated, the distance r between the source point and the field point tends to zero and singularities arise. The integral containing the term u_{ij}^{*} is weakly singular, with singularity of order $\ln(r)$. The integrals with the terms t_{ij}^{*} and u_{ijk}^{*} are strongly singular, with singularity order r^{-1} and the integral that contains the fundamental solution term t_{ijk}^{*} classifies as hyper-singular, due to the term r^{-2}. Thus, it is necessary to analyse them by methods that eliminate these singularities. Although there are several classical methods proposed and successfully applied to solve these integrals, the numerical implementation of these methods is laborious and often requires specific codes to handle each type of integral kernel. The method proposed by Gao [9], and presented in the section 2, allows evaluating all types of singular integrals kernels in a single numerical procedure, in a more direct way.Thus, it emerges as a powerful method to be used for new DBEM codes. However, no efforts in this direction is of our knowledge, so that a previous study of its efficiency and applicability to integrals of eq. (1) and eq. (2) is recommended. This is the main objective of the present paper.

As the intention is to apply the results obtained with DBEM in the analysis of fatigue crack propagation, based on the concepts of Linear Elastic Fracture Mechanics (LEFM) and using straight elements, it is necessary to correctly solve the integrals that appear in the analysis. Therefore, as a way of testing the method proposed by Gao [9], a computational code is implemented in Fortran 95 language, which solves the aforementioned singular integrals based on this formulation. The test variables and the methodology used are presented in section 3, while the numerical results obtained are found in section 4. Finally, the conclusion is presented in section 5.

2 Radial Polynomial Expansion Method

The method proposed by Gao [9] will be identified in this paper as the Radial Polynomial Expansion Method (RPEM) and allows the unified evaluation of any type of two-dimensional singular boundary integral. For this, RPEM proposes to express the non-singular parts of the integrand as polynomials of the distance r and then analytically remove those singularities. The formulation starts from two general singular integrals, which are:

$$I_i(\boldsymbol{\xi}) = \int_{\Gamma} f_i(\boldsymbol{\xi},\boldsymbol{x}) d\Gamma(\boldsymbol{x}) = \int_{\Gamma} \frac{\bar{f}_i(\boldsymbol{\xi},\boldsymbol{x})}{r^{\beta}(\boldsymbol{\xi},\boldsymbol{x})} d\Gamma(\boldsymbol{x}) \tag{3}$$

and

$$J_i(\boldsymbol{\xi}) = \int_{\Gamma} f_i(\boldsymbol{\xi},\boldsymbol{x}) d\Gamma(\boldsymbol{x}) = \int_{\Gamma} \frac{\bar{f}_i(\boldsymbol{\xi},\boldsymbol{x}) \ln[r(\boldsymbol{\xi},\boldsymbol{x})]}{r^{\beta}(\boldsymbol{\xi},\boldsymbol{x})} d\Gamma(\boldsymbol{x}), \tag{4}$$

where $\bar{f}_i(\boldsymbol{\xi},\boldsymbol{x})$ is bounded at any point in the domain or boundary, $r(\boldsymbol{\xi},\boldsymbol{x})$ is the distance between the source point ξ and the field point x and β indicates the level of singularity of the equations, so that:

$$
\begin{aligned}
&\beta = 0,\ I_i(\boldsymbol{\xi}) \text{ regular e } J_i(\boldsymbol{\xi}) \text{ weakly singular,}\\
&0 < \beta < 1,\ I_i(\boldsymbol{\xi}) \text{ weakly singular e } J_i(\boldsymbol{\xi}) \text{ strongly singular,}\\
&\beta = 1,\ I_i(\boldsymbol{\xi}) \text{ strongly singular e } J_i(\boldsymbol{\xi}) \text{ hyper-singular,}\\
&1 < \beta \leq 2,\ I_i(\boldsymbol{\xi}) \text{ hyper-singular e } J_i(\boldsymbol{\xi}) \text{ super-singular,}\\
&\beta > 2,\ I_i(\boldsymbol{\xi}) \text{ e } J_i(\boldsymbol{\xi}) \text{ super-singular.}
\end{aligned}
\tag{5}
$$

In order to remove the singularities, it is necessary to, initially, express the boundary differential $d\Gamma$ as a function of the radial distance differential dr, so that, after some mathematical manipulations:

$$
d\Gamma = \frac{dr}{\hat{r} \cdot \hat{l}}, \tag{6}
$$

where $\hat{r}$ is the unit vector of the distance r and $\hat{l}$ is the unit vector tangential to $d\Gamma$, according to Fig. 2.

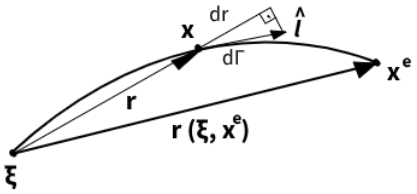

Figure 2. Variables in a singular element

Equation (6) is then substituted into eq. (3) and eq. (4), so that, for element e:

$$
I_i^e(\boldsymbol{\xi}) = \int_0^{r(\boldsymbol{\xi},\boldsymbol{x}^e)} \frac{\bar{f}_i(\boldsymbol{\xi},\boldsymbol{x})}{\hat{\boldsymbol{r}} \cdot \hat{\boldsymbol{l}} r^\beta(\boldsymbol{\xi},\boldsymbol{x})} dr(\boldsymbol{\xi},\boldsymbol{x}) \tag{7}
$$

and

$$
J_i^e(\boldsymbol{\xi}) = \int_0^{r(\boldsymbol{\xi},\boldsymbol{x}^e)} \frac{\bar{f}_i(\boldsymbol{\xi},\boldsymbol{x}) \ln[r(\boldsymbol{\xi},\boldsymbol{x})]}{\hat{\boldsymbol{r}} \cdot \hat{\boldsymbol{l}} r^\beta(\boldsymbol{\xi},\boldsymbol{x})} dr(\boldsymbol{\xi},\boldsymbol{x}), \tag{8}
$$

where the upper limit of the integrals, $r(\boldsymbol{\xi},\boldsymbol{x}^e)$, refers to the distance between the source point ξ and the final point x^e. This distance is represented in Fig. 2. For the solution of singular integrals, the non-singular part of the integrand is expanded into polynomials of r:

$$
\frac{\bar{f}_i(\boldsymbol{\xi},\boldsymbol{x})}{\hat{\boldsymbol{r}} \cdot \hat{\boldsymbol{l}}} = \sum_{n=0}^{N} C_i^n r^n(\boldsymbol{\xi},\boldsymbol{x}), \tag{9}
$$

where N is the order of the polynomials and C_i^n are the coefficients. These coefficients are obtained by placing the coordinate $\boldsymbol{x}$ at $N+1$ points between the source (ξ) and final (x^e) points, equally spaced by a distance ϵ. For the first point, $n = 0$, and therefore $\hat{\boldsymbol{r}} \cdot \hat{\boldsymbol{l}} = 1$, it is obtained that:

$$
C_i^0 = \bar{f}_i(\boldsymbol{\xi},\boldsymbol{\xi}). \tag{10}
$$

The other coefficients are obtained by:

$$\begin{bmatrix} 1 & r^1(\boldsymbol{\xi},\boldsymbol{x^1}) & ... & r^{N-1}(\boldsymbol{\xi},\boldsymbol{x^1}) \\ 1 & r^1(\boldsymbol{\xi},\boldsymbol{x^2}) & ... & r^{N-1}(\boldsymbol{\xi},\boldsymbol{x^2}) \\ \vdots & \vdots & & \vdots \\ 1 & r^1(\boldsymbol{\xi},\boldsymbol{x^N}) & ... & r^{N-1}(\boldsymbol{\xi},\boldsymbol{x^N}) \end{bmatrix} \begin{Bmatrix} C_i^1 \\ C_i^2 \\ \vdots \\ C_i^N \end{Bmatrix} = \begin{Bmatrix} (\bar{f}_i(\boldsymbol{\xi},\boldsymbol{x^1})/(\hat{\boldsymbol{r}}\cdot\hat{\boldsymbol{l}}) - C_i^0)/r(\boldsymbol{\xi},\boldsymbol{x^1}) \\ (\bar{f}_i(\boldsymbol{\xi},\boldsymbol{x^2})/(\hat{\boldsymbol{r}}\cdot\hat{\boldsymbol{l}}) - C_i^0)/r(\boldsymbol{\xi},\boldsymbol{x^2}) \\ \vdots \\ (\bar{f}_i(\boldsymbol{\xi},\boldsymbol{x^N})/(\hat{\boldsymbol{r}}\cdot\hat{\boldsymbol{l}}) - C_i^0)/r(\boldsymbol{\xi},\boldsymbol{x^N}) \end{Bmatrix}, \tag{11}$$

where x^n represents the coordinate of the point $(n+1)$.

Substituting eq. (9) in eq. (7) and performing the necessary mathematical manipulations, the method then returns the solution of the integral I_i^e, so that:

$$I_i^e(\boldsymbol{\xi}) = \sum_{n=0}^{N} C_i^n F^n, \tag{12}$$

where:

$$F^n = \begin{cases} \frac{r^{n-\beta+1}(\boldsymbol{\xi},\boldsymbol{x^e})}{n-\beta+1} & \text{for } n-\beta+1 \neq 0 \\ \\ \ln[r(\boldsymbol{\xi},\boldsymbol{x^e})] & \text{for } n-\beta+1 = 0 \end{cases}. \tag{13}$$

The integral J_i^e of eq. (8) can be solved similarly, resulting in:

$$J_i^e(\boldsymbol{\xi}) = \sum_{n=0}^{N} C_i^n H^n, \tag{14}$$

where:

$$H^n = \begin{cases} \frac{-\{a\ln[r(\boldsymbol{\xi},\boldsymbol{x^e})]+1\}}{a^2 r^a(\boldsymbol{\xi},\boldsymbol{x^e})} & \text{for } a = \beta-n-1 \neq 0 \\ \\ \frac{1}{2}\{\ln[r(\boldsymbol{\xi},\boldsymbol{x^e})]\}^2 & \text{for } a = \beta-n-1 = 0 \end{cases}. \tag{15}$$

According to Gao [9], eq. (12) and eq. (14) can be used in the evaluation of singular integrals of arbitrary order. If the singular integral exists, the equations return the result in the Cauchy Principal Value. If the integral does not exist, the finite part of the result is returned.

3 Formulation

In order to evaluate the reliability of the RPEM and the applicability of the method in DBEM, it is proposed the analysis of an element with quadratic interpolation functions, initially straight, and discontinuous, with $\lambda_1 = \lambda_2 = 2/3$, i.e., the extreme nodes are located at points $\eta = -2/3$ and $\eta = +2/3$, instead of $\eta = -1$ and $\eta = +1$. To evaluate the behaviour of the method in the analysis of curved elements, the source point 2 ($\boldsymbol{\xi}_2$) of the straight element is slightly moved in 5 steps, until reaching the maximum proposed distortion, in which the coordinates of $\boldsymbol{\xi}_2$ are (1.5, 2.5). The straight element and the element with maximum distortion studied are shown in Fig. 3. It is considered a plane strain state, with an elasticity modulus of 26710.3 MPa and Poisson's ratio equal to 0.245.

To carry out the tests, the RPEM formulation is implemented in a computational program coded in Fortran 95 language. Then, the integrals kernels composed by the fundamental solution terms u_{ij}^*, t_{ij}^* and t_{ijk}^* ate tested

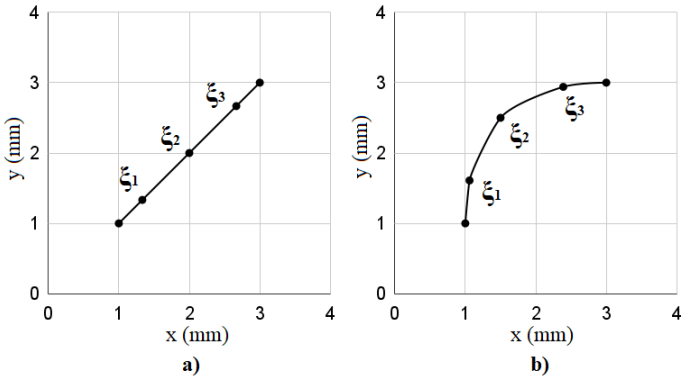

Figure 3. Elements used in the analysis, being a) straight, b) with maximum distortion

for different quantities of expansion polynomials, ranging from 3 to 15 polynomials, yielding 7 results. The integrals containing the term u^*_{ijk} are not evaluated here, since the crack faces are assumed to be traction-free. For comparative purposes, the results of these same integrals are calculated by the Singularity Subtraction Method (SSM), a method that is widely disseminated for solving singular integrals. In the SSM application, based on Aliabadi [7], Kzam [10] and Aliabadi and Hall [11], three different results are generated, associated to truncation at different orders of the interpolation functions, $N_\alpha(\eta)$, series expansion, i.e., using one, two or three terms from

$$N_\alpha(\eta) \approx N_\alpha(\eta_0) + \frac{\partial N_\alpha}{\partial \eta}(\eta_0)[\eta - \eta_0] + \frac{1}{2}\frac{\partial^2 N_\alpha}{\partial \eta^2}(\eta_0)[\eta - \eta_0]^2, \tag{16}$$

keeping the other terms present in the integrand truncated at the zero-order term.

Integrals with weakly singular kernels (u^*_{ij}) are analysed for the straight element and for all five curved elements. On the other hand, strongly singular (t^*_{ij}) and hyper-singular (t^*_{ijk}) integrals kernels are analysed for the straight element only, since crack propagation analyses by DBEM are usually performed by adding straight segments (elements). The seven results obtained by the RPEM and the three results obtained by the SSM are then compared with numerical and analytical results. This comparison is made by calculating the percentage error of the results obtained by RPEM and SSM, based on the values obtained numerically by logarithmic quadrature for u^*_{ij} and analytically for straight elements (see [12]) for t^*_{ij} and t^*_{ijk}. The results of such comparisons are presented in the section 4 below.

4 Numerical Results

Tables 1 to 6 summarize the errors obtained for each analysis, considering the reference results (logarithmic quadrature with 12 integration points for u^*_{ij} and analytical results for t^*_{ij} and t^*_{ijk}). Noting that u^*_{ij} and t^*_{ij} correspond to four components and t^*_{ijk} corresponds to six components, only the maximum error, in each case, is reported. The presentation of the results related to SSM is divided into 3 columns, which differ due to the expansion adopted for the interpolation function. The presentation of the results related to the RPEM are divided into 7 columns, related to the number of expansion polynomials (N) used in the analysis.

First, the integral u^*_{ij} is analysed. In Table 1 the absolute maximum errors are presented, in percentage, when comparing the results obtained with the SSM and the results expected by the logarithmic quadrature. In Table 2, the comparison is performed between RPEM and logarithmic quadrature.

The analysis of the integral t^*_{ij} is performed for the straight element. Thus, in Table 3, it is presented the absolute maximum errors, in percentage, comparing the results obtained with the SSM and the expected analytical results. The comparison is then repeated for the results obtained with the RPEM and displayed in Table 4.

Also analysing the straight element for the integral t^*_{ijk}, it is shown in Table 5 the absolute maximum errors, in percentage, between the results obtained by SSM and the analytical ones, while in Table 6 the results obtained by RPEM are compared.

Table 1. Absolute maximum error (%) when comparing the results for the integral u^*_{ij} obtained with SSM and logarithmic quadrature (with 12 integration points)

Element	N_α truncated at 1st term	N_α truncated at 2nd term	N_α fully expanded
Straight	3.534	0.471	0.463
$\boldsymbol{\xi}_2$ (1.9, 2.1)	3.881	0.554	0.520
$\boldsymbol{\xi}_2$ (1.8, 2.2)	4.417	0.693	0.630
$\boldsymbol{\xi}_2$ (1.7, 2.3)	5.215	0.981	0.809
$\boldsymbol{\xi}_2$ (1.6, 2.4)	6.387	1.934	1.085
$\boldsymbol{\xi}_2$ (1.5, 2.5)	13.342	13.342	1.503

Table 2. Absolute maximum error (%) when comparing the results for the integral u^*_{ij} obtained with RPEM and logarithmic quadrature (with 12 integration points)

Element	N = 3	N = 5	N = 7	N = 9	N = 11	N = 13	N = 15
Straight	0	0	0	0	2.503E-06	8.599E-05	3.152E-03
$\boldsymbol{\xi}_2$ (1.9, 2.1)	0.099	7.652E-04	1.805E-05	0	3.092E-06	5.053E-05	3.021E-03
$\boldsymbol{\xi}_2$ (1.8, 2.2)	0.235	0.021	1.561E-03	8.876E-05	8.069E-06	2.824E-05	2.243E-03
$\boldsymbol{\xi}_2$ (1.7, 2.3)	0.491	0.194	0.027	3.411E-03	4.165E-04	1.203E-04	3.772E-03
$\boldsymbol{\xi}_2$ (1.6, 2.4)	2.487	1.055	0.243	0.052	0.011	2.504E-03	0.010
$\boldsymbol{\xi}_2$ (1.5, 2.5)	14.744	4.319	1.488	0.493	0.163	0.054	7.480E-03

Table 3. Absolute maximum error (%) when comparing the results for the integral t^*_{ij} obtained with SSM and analytically by Portela [12]

Element	N_α truncated at 1st term	N_α truncated at 2nd term	N_α fully expanded
Straight	0	0	0

Table 4. Absolute maximum error (%) when comparing the results for the integral t^*_{ij} obtained with RPEM and analytically by Portela [12]

Element	N = 3	N = 5	N = 7	N = 9	N = 11	N = 13	N = 15
Straight	0	0	0	0	0	1.204E-05	1.191E-04

Table 5. Absolute maximum error (%) when comparing the results for the integral t^*_{ijk} obtained with SSM and analytically by Portela [12]

Element	N_α truncated at 1st term	N_α truncated at 2nd term	N_α fully expanded
Straight	870.079	0	0

Table 6. Absolute maximum error (%) when comparing the results for the integral t^*_{ijk} obtained with RPEM and analytically by Portela [12]

Element	N = 3	N = 5	N = 7	N = 9	N = 11	N = 13	N = 15
Straight	0	0	0	0	1.347E-06	2.829E-05	3.124E-03

It is possible to see from Table 1 and Table 2 that, for the integral involving u^*_{ij}, the Radial Polynomial Expansion Method, proposed by Gao [9], proved to be more efficient, if only zero-order terms are considerer in the SSM. It is possible to obtain, with the RPEM, the exact value that is expected by the logarithmic quadrature,

using the minimum number of terms in the expansion, for a straight element. For curved elements, the RPEM starts to present larger errors for N = 3, but these errors drop considerably as the number of polynomial terms in the expansion is increased. In SSM, however, even when completely expanding the interpolation function, the values obtained are not as close to those of logarithmic quadrature as those of RPEM, always presenting errors greater than this last method. Thus, the SSM proves to be more laborious than the RPEM, being necessary to carry out the expansion of other quantities involved in the integral kernel. In the analysis of the integral that contains t^*_{ij}, both the RPEM and the SSM were able to provide the exact result that was expected analytically, in the most basic format of their formulations, the SSM being with the interpolation function truncated in the first term and the method of Gao [9] with 3 polynomial terms of expansion. As for the integral that contains t^*_{ijk}, the two methods also met the requirement, finding the exact expected value, but RPEM achieved this in its basic formulation, while SSM was more laborious, and it was necessary to expand the interpolation function at least up to the second term.

5 Conclusions

The method proposed by Gao [9], called in this paper as Radial Polynomial Expansion Method, presents satisfactory results in the analysis of straight elements. This is because it is possible to obtain the exact result expected by other numerical and analytical formulations, for all the studied integrals, with the minimum number of polynomial terms proposed, i. e., N $= 3$. Moreover, solving weakly singular integrals (which kernel contains u^*_{ij} terms) over distorted elements, while the singularity subtraction technique requires higher order terms of each kernel component (which is a laborious task) for reliable results, the RPEM only requires the increase of the number of polynomial terms to improve the results.

As the proposed objective is to apply the results of these integrals in a code for fatigue crack propagation problems, using straight elements, the RPEM presents reliable results and is applicable in the solution of LEFM problems through DBEM.

Acknowledgements. The authors acknowledge the support by the Brazilian agencies CAPES and CNPq (Grant number: 405548/2021-4).

Authorship statement. The authors hereby confirm that they are the sole liable persons responsible for the authorship of this work, and that all material that has been herein included as part of the present paper is either the property (and authorship) of the authors, or has the permission of the owners to be included here.

References

[1] H. Hong and J. Chen. Derivations of integral equations of elasticity. *J. Eng. Mech*, vol. 114, pp. 1028–1044, 1988.

[2] A. Portela, M. H. Aliabadi, and D. P. Rooke. Dual boundary element analysis of cracked plates: singularity subtraction technique. *International Journal of Fracture*, vol. 55, pp. 17–28, 1992a.

[3] A. Portela, M. H. Aliabadi, and D. P. Rooke. The dual boundary element method: effective implementation for crack problems. *International Journal for Numerical Methods in Engineering*, vol. 33, pp. 1269–1287, 1992b.

[4] A. Portela, M. H. Aliabadi, and D. P. Rooke. Dual boundary element incremental analysis of crack propagation. *Computers & Structures*, vol. 46, n. 2, pp. 237–247, 1993.

[5] C. A. Brebbia, J. C. F. Telles, and L. C. Wrobel. *Boundary Elements Techniques: Theory and Applications in Engineering*. Springer-Verlag, Berlin, 1984.

[6] C. A. Brebbia. *Boundary Elements: An Introductory Course*. WIT Press/Computational Mechanics Publications, Boston/Southampton, 1992.

[7] M. H. Aliabadi. *The boundary element method. Applications in solids and structures*. John Wiley & Sons Inc, Chichester, 2002.

[8] J. T. Katsikadelis. *Boundary Elements: Theory and Applications*. Academic Press - Elsevier, 2016.

[9] X.-W. Gao. Numerical evaluation of two-dimensional singular boundary integrals - theory and fortran code. *Journal of Computational and Applied Mathematics*, vol. 188, pp. 44–64, 2006.

[10] A. K. L. Kzam. Formulação dual em mecânica da fratura utilizando elementos de contorno curvos de ordem qualquer. Master's thesis, Universidade de São Paulo, São Carlos, SP, Brasil, 2009.

[11] M. H. Aliabadi and W. Hall. Two-dimensional boundary element kernel integration using series expansions. *Engineering Analysis with Boundary Elements*, vol. 6, pp. 140–143, 1989.

[12] A. Portela. *Dual boundary element analysis of crack growth*. Computational Mechanics Publications: Topics in engineering, Southampton, UK and Boston, USA, 1993.